Author Manuscript

Author Manuscript

Author Manuscript

Author Manuscript

HHS Public Access

Author manuscript

Life Sci. Author manuscript; available in PMC 2020 May 01.

Published in final edited form as:

Life Sci. 2019 May 01; 224: 187–196. doi:10.1016/j.lfs.2019.03.035.

Antioxidant and immunomodulatory activity induced by stevioside in liver damage: *in vivo, in vitro* and *in silico* assays.

Sael Casas-Grajales[a], **Erika Ramos-Tovar**[a], **Esmeralda Chávez-Estrada**[b], **Diana Alvarez-Suarez**[a], **Erika Hernández-Aquino**[a], **Karina Reyes-Gordillo**[d,e], **Carlos M. Cerda-García-Rojas**[b], **Javier Camacho**[a], **Víctor Tsutsumi**[c], **M. Raj Lakshman**[d,e], and **Pablo Muriel**[a,*]

[a]Department of Pharmacology, Cinvestav-IPN, Av. Instituto Politécnico Nacional 2508, Col. San Pedro Zacatenco, 07360, Apartado Postal 14-740, Mexico City, Mexico.

[b]Department of Chemistry, Cinvestav-IPN, Av. Instituto Politécnico Nacional 2508, Col. San Pedro Zacatenco, 07360, Apartado Postal 14-740, Mexico City, Mexico.

[c]Department of Infectomics and Molecular Pathogenesis, Cinvestav-IPN, Av. Instituto Politécnico Nacional 2508, Col. San Pedro Zacatenco, 07360, Apartado Postal 14-740, Mexico City, Mexico.

[d]Department of Biochemistry and Molecular Biology, School of Medicine and Health Science, The George Washington University Medical Center, 2300 I St NW, Washington, DC 20052, EE. UU.

[e]Lipid Research Laboratory, VA Medical Center, 50 Irving St, Washington, DC 20422, EE. UU.

Abstract

Aims: Stevioside is a diterpenoid obtained from the leaves of *Stevia rebaudiana* (Bertoni) that exhibits antioxidant, antifibrotic, antiglycemic and anticancer properties. Therefore, we aimed to study whether stevioside has beneficial effects in liver injury induced by long-term thioacetamide (TAA) administration and investigated the possible underlying molecular mechanism using *in vivo*, *in vitro* and *in silico* approaches.

Main methods: Liver injury was induced in male Wistar rats by TAA administration (200 mg/kg), intraperitoneally, three times per week. Rats received saline or stevioside (20 mg/kg) twice daily intraperitoneally. In addition, cocultures were incubated with either lipopolysaccharide or ethanol. Liver injury, antioxidant and immunological responses were evaluated.

Key findings: Chronic TAA administration induced significant liver damage. In addition, TAA upregulated the protein expression of nuclear factor (NF)-κB, thus increasing the expression of proinflammatory cytokines and decreasing the antioxidant capacity of the liver through downregulation of nuclear erythroid factor 2 (Nrf2). Notably, stevioside administration prevented

*Corresponding author: Laboratory of Experimental Hepatology, Department of Pharmacology, Cinvestav-IPN, Av. Instituto Politécnico Nacional 2508, Col. San Pedro Zacatenco, 07360, Apartado Postal 14-740, Mexico City, Mexico. pmuriel@cinvestav.mx; Telephone: +52-55-57473303; Fax: +52-55-57473394.

Publisher's Disclaimer: This is a PDF file of an unedited manuscript that has been accepted for publication. As a service to our customers we are providing this early version of the manuscript. The manuscript will undergo copyediting, typesetting, and review of the resulting proof before it is published in its final citable form. Please note that during the production process errors may be discovered which could affect the content, and all legal disclaimers that apply to the journal pertain.

Conflict of interest:
The authors declare that they have no conflicts of interest.

Author Manuscript Author Manuscript Author Manuscript Author Manuscript

all of these changes. *In vitro*, stevioside prevented the upregulation of several genes implicated in liver inflammation when cocultured cells were incubated with lipopolysaccharide or ethanol. *In silico* assays using tumor necrosis factor receptor (TNFR)-1 and Toll-like receptor (TLR)-4-MD2 demonstrated that stevioside docks with TNFR1 and TLR4-MD2, thus promoting an antagonistic action against this proinflammatory mediator.

Significance: Collectively, these data suggest that stevioside prevented liver damage through antioxidant activity by upregulating Nrf2 and immunomodulatory activity by blocking NF-κB signaling.

Keywords

TAA; stevioside; docking; immunomodulatory; cocultures; Nrf2

1 Introduction

Stevioside is a noncaloric sweetener extracted from the leaves of *Stevia rebaudiana* (Bertoni). Stevioside is a diterpenoid glycoside that is 300 times sweeter than sucrose and exhibits several pharmacological properties, such as antioxidant, anti-inflammatory, antitumor, and antidiabetic properties, that can be beneficial for fighting liver injury [1, 4–7]. The safety profile of stevioside has been evaluated by the Joint Food and Agricultural Organization and the World Organization Expert Committee on Food Additives and has been used in the food industry since 2011 (1–4).

On the other hand, thioacetamide (TAA) is a strong hepatotoxin that is useful to induce fibrosis and cirrhosis within a short period of time; therefore, it is a powerful tool to study compounds with possible beneficial effects on the liver (5). Because rats are not susceptible to developing chronic liver injury induced by ethanol (EtOH) administration, which is a major cause of human-induced liver damage, we decided to use an experimental model based on cell cultures exposed to EtOH. Therefore, we decided to use the recombinant cell line VL-17A, which is a HepG2 cell line that constitutively expresses CYP2E1 (of human origin) and alcohol dehydrogenase (ADH, of murine origin) genes (6). Moreover, we wanted to explore the anti-inflammatory effect of stevioside; therefore, we exposed VL-17A cells to lipopolysaccharides (LPSs), which are extensively used to study the immune system because they cause the release of proinflammatory cytokines, such as tumor necrosis factor-α (TNF-α), interleukin-(1β), and IL-6, and increase the production of reactive nitrogen species, inducing liver damage (5,7). Therefore, we aimed to investigate whether stevioside was able to prevent TAA-induced liver inflammation and the oxidative stress response in rats and if so, to search for the mechanisms involved by using *in vivo*, *in vitro* and *in silico* assays.

2 Materials and methods

2.1 Animal study design

The animal protocol was approved (No. 269–05; 11 January 2014) by the appropriate institutional committee, which was the Unit of Production and Experimentation of Laboratory Animals (UPEAL), at the Center for Research and Advanced Studies of the National Polytechnic Institute (Cinvestav-IPN). In addition, this protocol complied with the

Author Manuscript Author Manuscript Author Manuscript Author Manuscript

Mexican official regulations (NOM-062-ZOO-1999) and the National Institutes of Health Guide for the Care and Use of Laboratory Animals (NIH Publications No. 8023, revised 1978). For *in vivo* studies, Wistar male rats obtained from the UPEAL and weighing 100–120 g upon arrival were utilized. The animals were acclimatized for one week. Then, the animals were housed in polycarbonate cages under controlled conditions (21±1 °C, 50–60% relative humidity, and 12-h dark-light cycles), fed Purina® rat chow and provided water *ad libitum*. Four groups (n=8) of rats were formed. Liver fibrosis was produced by TAA (200 mg/kg of body weight, i.p.) administration three times per week for 8 weeks. Stevioside (20 mg/kg, of body weight, i.p.) was administered twice per day during TAA treatment. The vehicle, TAA and stevioside groups received treatments accordingly. Animals were euthanized under light ketamine/xylazine anesthesia, and the liver and blood were rapidly obtained. All samples were stored at −70 °C until analysis.

2.2 Cell lines and culture conditions

Human HSCs (hHSCs) were obtained from hepatic biopsy patients with obesity as previously described in detail (8,9) VL-17A cells were kindly provided by Dr. Dahn L. Clemens. The main characteristic of these cells is that they express murine class I ADH from the expression vector pIV-G2, which contains the coding region of the human cytochrome CYP2E1. For detailed information, the reader is referred to (6). We utilized hHSC and VL-17A cells cocultured at a ratio of 1:10 to simulate *in vivo* conditions (10). The cells were grown to semiconfluence in DMEM-F12 supplemented with 10% (v/v) FBS, 1% (v/v) penicillin/streptomycin, 5 mg/L ITS and dexamethasone 10^{-7} M, 5 μL/10 mL neomycin, 4 μL/1 mL zeocin, and 8 μL/1 mL G418. The medium was replaced with DMEM-F12 with reduced FBS (0.1%, v/v) to synchronize cell activity, and the cocultures were treated with Reb A at concentrations of 1, 5, 10, 20 and 100 mM and with 200 μL/20 mL (1 mg/1 mL) LPS or 100 mM EtOH plus Reb A at 37 °C and 5% CO_2 for 18 h. This coculture model has previously been characterized and utilized by our group; the reader is referred to (11) for more information.

2.3 Serum enzyme activities

Blood samples were centrifuged at 1,200 × g for 15 min to collect the serum. Then, liver damage was assessed by measuring the activities of alanine aminotransferase (ALT) (12), γ-glutamyl transpeptidase (γ-GTP) (13) and alkaline phosphatase (ALP) (14).

2.4 Histology

Liver sections were taken from all the animals and fixed with 10% formaldehyde in PBS for 24 h. Tissue samples were washed with tap water, dehydrated in alcohol, and embedded in paraffin. Five-micrometer-thick sections were mounted on glass slides covered with silane. Staining was performed with hematoxylin and eosin (H&E).

2.5 Glycogen determination

The Seifter and Dayton method was followed with the anthrone reagent (15). The absorbance of the samples was read at 620 nm, and appropriate glucose standards were prepared.

Author Manuscript Author Manuscript Author Manuscript Author Manuscript

2.6 Western blot assays

Western blot assays were performed as previously described (16). Volumes equivalent to 50 and 120 μg of protein were loaded into wells of 15, 12, and 10% polyacrylamide gels. Separated proteins were transferred onto an Immuno-Blot™ PVDF membrane (BIO-RAD, Hercules, CA, USA). Then, blots were blocked for 1 or 2 h at room temperature and incubated independently overnight at 4 °C with the following primary antibodies: IL-6 and IL-10 (Invitrogen, Waltham, MA, USA), IL-1β and nuclear factor (NF)-κB (EMD Millipore, Billerica, MA, USA), TNF-α, IL-17a (Santa Cruz, Santa Cruz, CA, USA) and nuclear factor (erythroid-derived 2)-like2 (Nrf2; Abcam, Cambridge, MA, USA), then exposed to a secondary peroxidase-labeled antibody in blocking solution at room temperature for 2 h. Blots were stripped and incubated with a monoclonal antibody against β-actin (Ambion, Austin, TX, USA) and used as a control to normalize cytokine protein expression levels. Images were digitalized and then analyzed densitometrically using ImageJ® software (National Institutes of Health, Bethesda, MD, USA).

2.7 Immunohistochemistry assays

Immunohistochemical (IHC) staining was performed by using an immunoperoxidase protocol. Sections were dewaxed overnight at 58 °C. The specimens were hydrated in xylene (3 × 5 min) and 90% alcohol (4 × 3 min). Subsequently, sections were submerged in 1x PBS (3 × 5 min), autoclaved with 0.10 N citrate buffer at 121 °C for 20 min, and washed again with 1x PBS (3 × 5 min). Subsequently, endogenous peroxidase was blocked with methanol (46 mL of MeOH+ 4 mL of H_2O_2) for 60 min, followed by five washes in 1x PBS for 5 min. Furthermore, to block nonspecific binding, 5% milk in 1x PBS was added for 60 min. The tissues were then rinsed with 1x PBS for 5 × 5 min. Subsequently, the tissues were incubated with a primary antibody against nuclear factor (NF)-κB (EMD Millipore, Billerica, MA, USA) diluted in 3% fetal bovine serum overnight and rinsed with 1x PBS (5 × 5 min). The tissues were incubated with the secondary antibody for 2 h at 18–21 °C (room temperature) and then rinsed with 1x PBS (5 × 5 min). Four hundred microliters of the peroxidase substrate 3,3′-diaminobenzidine ((DAB); 40 μL DAB in 360 μL H_2O_2) was added, incubated for 45 min, and rinsed with 1x PBS (5 × 5 min). Finally, the stained sections were counterstained with hematoxylin for 1 min and rinsed with 1x PBS (2 × 5 min), and the tissues were dehydrated in alcohol (4 × 80 s) and xylene (3 × 5 min). The stained specimens were covered with resin and allowed to dry for 2 days. All stained sections were visualized by using a light microscope (80i, Eclipse, Nikon, Tokyo, Japan). Brown staining of proteins in the tissue sections was considered a positive reaction. Digital images of the histological sections were collected, and a positive signal was quantified by using ImageJ® software (NIH, MD, USA) (16).

2.8 DPPH· inhibition assay

The antioxidant activity of stevioside was measured using DPPH·, as previously described (17). In summary, Reb A dissolved in EtOH at various concentrations was added to a tube containing 2 mL of a 0.1 mM solution of DPPH· in EtOH. The absorbance was measured at 517 nm using a spectrometer (PerkinElmer Lambda 2S UV/Vis) at different time points. As

Author Manuscript Author Manuscript Author Manuscript Author Manuscript

a positive control and for comparison purposes, quercetin (Sigma-Aldrich St Louis, Missouri, USA) was utilized.

2.9 Assessment of lipid peroxidation

The extent of lipid peroxidation (LPO) was measured in liver homogenates by taking into account the amount of malondialdehyde (MDA) formation using the thiobarbituric acid method (18). Proteins were determined according to the Bradford assay (19), using bovine serum albumin as a standard.

2.10 RNA isolation and quantitative RT-qPCR assays

Total RNA isolation was performed as previously described (16). qPCR was performed using the Applied Biosystems™ StepOnePlus Real-Time PCR system. Taq polymerase (TaqMan, Universal Master Mix Prod # 4304437, Applied Biosystems, CA, USA) was used for the analysis of the relative expression of NF-κB (Rn01502266_m1), IL-1β (Rn00580432_m1), TNF-α (Rn01525859_g1), IL-6 (Rn01410330_m1), and IL-10 (Rn00563409_m1). Probes were purchased from Thermo Fisher Scientific. A no template control, a target reagent sample, and a negative sample were included on the plate. GAPDH (Rn01775763_g1) was used as the internal control, and the relative gene expression was calculated using the Livak method (20).

2.11 Conformational analysis

The molecular structure of stevioside was obtained from the SuperSweet database (#42576) (21) (http://bioinformatics.charite.de/sweet/) and corroborated using the template from the PubChem database of Avogadro version 1.2, which is an open-source molecular builder and visualization tool (22). Using the same software, an extensive conformational search was performed using the systematic rotor search, which was carried out with a population contribution cutoff of 1×10^{-7} and by applying the MMFF94 force field (23) calculation. After analysis of the geometry, the conformer with the lowest energy and highest population contribution was optimized by DFT geometry optimization at the B3LYP/DGDZVP level of theory, employing the Gaussian 09W software program revision B.01 (Gaussian Inc., Wallingford, CT, USA) (24).

2.12 Docking study.

The stevioside minimum energy molecular model described above was utilized as the starting point for ligand preparation. Default values were assigned for the ligand, torsion tree and the Gasteiger-Marsili charges by means of the AutoDock 4.2.6 software (The Scripps Research Institute, La Jolla, CA, USA) (25). Docking was carried out with the crystallographic files of the TLR4-MD2 (2Z65) (26) and TNFR1 (1FT4) (27) receptors that were obtained from the RCSB Protein Data Bank. *In silico* simulations were performed on a computer equipped with an Intel® Core™ i7–2620m CPU at 2.70 GHz with an HD Intel®3000 integrated video card and 4 GB of RAM. The results were visualized and analyzed with AutoDock Tools 4.2 (The Scripps Research Institute, La Jolla, CA, USA), PyMOL 2.1 (Schrödinger, New York, NW, USA), and BIOVIA Discovery Studio 2018 (BIOVIA, San Diego, CA, USA) programs for Windows.

Author Manuscript Author Manuscript Author Manuscript Author Manuscript

2.13 Statistical analysis

All data are expressed as the mean values ± SEM. Comparisons were carried out by 1-way analyses of variance, followed by a post hoc Tukey's Honest Significant Difference test, as appropriate, using GraphPad Prism version 6.0 for Windows (La Jolla, CA, USA; www.graphpad.com). Differences were considered statistically significant when P was ≤ 0.05.

3 Results

3.1 Stevioside prevents morphological and biochemical alterations in the livers of TAA-treated rats

To determine the alterations induced by chronic administration of TAA in liver parenchyma, liver macroscopic and microscopic images were taken from all groups. As shown in Fig. 1A–H, TAA treatment (Fig. 1B and F) altered liver morphology and disrupted liver parenchyma compared with the control group (Fig. 1A and E), resulting in the presence of regenerative hepatocyte nodules and some necrotic cells (28). Notably, as shown in Fig. 1C and G, the administration of stevioside markedly prevented the morphological and histological changes caused by TAA administration. Stevioside treatment in control rats had no effect on general liver appearance or histology (Fig. 1D and H).

Body weight gain decreased in the chronic TAA intoxication group compared with the control group (Fig. 2A, B, and C), and stevioside was unable to preserve body weight gain. The liver weight in the cirrhotic group decreased compared with the liver weight in the control group (Fig. 2D), and stevioside did not produce a significant effect on the liver weight decrement produced by TAA. The liver/body weight ratio increased with chronic TAA administration (Fig. 2E), and stevioside administration did not prevent this increase.

Next, we assessed the glycogen content in the livers of treated rats. As shown in Fig. 1N, TAA-treated rats exhibited very low levels of glycogen, and stevioside coadministration partially prevented this diminution, indicating that this compound significantly preserved liver functionality (Fig. 2F). In addition, serum enzymatic activities of ALT (Fig. 2G), γ-GTP (Fig. 2H) and ALP (Fig. 2I) were significantly increased in the TAA-treated rats, as previously reported (16). The administration of stevioside in control rats did not produce any effects.

3.2 Stevioside prevents TAA-induced liver damage induced by blocking NF-κB and proinflammatory cytokines

Fig. 3 shows that few p65-specific antigens were detected in the control group (Fig. 3A). In contrast, the expression of p65 was significantly higher in the TAA group (Fig. 3B) compared to the control group. Notably, stevioside cotreatment significantly ameliorated the induced upregulation of p65 (Fig. 3C) compared to the induced upregulation of p65 in cirrhotic animals. Fig. 3E shows the percentage of zones of positivity obtained from the 3 liver slices. The results were confirmed by qRT-PCR (Fig. 3F) and by WB (Fig. 3G), which showed that TAA induced a significant increase in p65 mRNA and protein levels, while

Author Manuscript Author Manuscript Author Manuscript Author Manuscript

stevioside treatment significantly attenuated this effect. Stevioside treatment in control rats had no effect on p65.

As shown in Fig. 4, IL-17a (A), IL-1β (B, C), TNF-α (D, E), IL-6 (F, G) and IL-10 (H, I) mRNA and protein levels were significantly increased by chronic TAA treatment; it is worth noting that stevioside cotreatment significantly prevented the elevation of all of these proinflammatory cytokines. Stevioside treatment in control rats did not produce any effect.

3.3 Stevioside improves the cellular redox state by preserving Nrf2 rather than by free radical scavenging activity

To investigate whether stevioside is a good antioxidant, a radical scavenging assay was performed. As shown in Fig. 5A, stevioside displayed weak, concentration-dependent antioxidant activity when compared with the well-known antioxidant quercetin. Then, we wanted to explore the possibility that stevioside protects cells from oxidative stress by improving the endogenous antioxidant system that is regulated through the Nrf2 pathway (29). As shown in Fig. 5B, the TAA-treated group showed decreased levels of liver Nrf2 compared with the control group. Notably, stevioside preserved the Nrf2 protein levels. Most notably, as a result of the preservation of normal Nfr2 levels by stevioside, the elevation of membrane markers of oxidative stress, such as LPO (Fig. 5D) was prevented by cotreatment with stevioside. In addition, the liver GSH concentration (Fig. 5C), as well as GPx mRNA levels (Fig. 5E) that were decreased by TAA treatment, showed normal values when rats were protected by coadministration with stevioside. Fig. 5F and G show the chemical formulas of quercetin and stevioside, respectively. Stevioside treatment in control rats did not exhibit any effect.

3.4 Stevioside prevents the upregulation of proinflammatory genes induced by LPS or EtOH in cocultured cells

Although TAA shares some characteristics with alcohol-induced liver damage and exhibits some degree of inflammation, we decided to use EtOH in cultured cells because it is the etiological agent most consumed in the world; moreover, LPS is considered an excellent inducer of an exacerbated immunological reaction; thus, we utilized LPS to investigate the anti-inflammatory and immunomodulatory activity of stevioside. Therefore, to confirm the *in vivo* results, the anti-inflammatory properties were also characterized in cocultures of hHSC/VL-17A cells. As shown in Fig. 6A and B, incubation of cocultures with LPS or EtOH increased the levels of NF-κB mRNA compared with the control group, and stevioside administration significantly prevented this increase. As expected, the mRNA levels of proinflammatory cytokines regulated by NF-κB, TNF-α (Fig. 6C and D), and IL-6 (Fig. 6E and F) increased with LPS or EtOH incubation, and incubation with stevioside partially or completely prevented these elevations. In all cases, stevioside incubation alone exhibited no effect.

3.5 Docking studies show a possible immunoregulatory mechanism of stevioside.

Molecular docking is mainly used as a predictive tool to anticipate the possible molecular interactions between proteins and ligands at the atomic level, which allows researchers to characterize the behavior of the ligand in the binding site of the target proteins as well as to

Author Manuscript Author Manuscript Author Manuscript Author Manuscript

understand fundamental biochemical processes (30). As shown in Fig. 7A, stevioside exhibits low binding energy of −0.9 kcal/mol to TNFR1, which implies a slight impediment of stevioside binding to the receptor. As shown in Fig. 7B and C, stevioside binds to amino acids PHE60, THR61, ALA62, LEU67, and LEU71, which are implicated in TNFR1 inhibition. Moreover, as shown in Fig. 7D–F, stevioside and the TNFR1 inhibitor, IV703, were superimposed, and both molecules matched.

As shown in Fig. 8A, when stevioside was docked with the TLR4-MD2 complex, the binding energy was −5.6 kcal/mol, which is higher than energy observed when docked with TNFR1, suggesting a better affinity for the receptor complex. As shown in Fig. 8B and C, the amino acids binding with stevioside are ILE63, PHE76, TYR102, ILE117, PHE119, SER120, PHE121, LYS122, and PHE151, which are targets for LPS pathway inhibition. As shown in Fig. 8D–F, when stevioside was superimposed over the inhibitor control (Eritoran), both matched in the pocket corresponding to MD-2.

4 Discussion

In the present work, we found that stevioside prevented TAA-induced liver damage and inflammation by downregulating NF-κB and proinflammatory cytokines and upregulating Nrf2, thus preserving the normal cell redox status. Because rats display a natural aversion to EtOH, the most frequently used substance that produces liver damage in humans, and since LPS is the most suitable substance to study the immunomodulatory activity of a given compound, the *in vivo* effects of EtOH and LPS were corroborated utilizing VL-17A cells cocultured with hHSCs incubated with LPS or EtOH. The results suggested that the pharmacological effects of stevioside on the liver are associated with its ability to modulate NF-κB signaling. In addition, *in silico* assays suggested that the effects afforded by stevioside are associated, at least in part, with its immunomodulatory properties driven by binding to receptors that activate the NF-κB pathway.

Previously, we performed a preliminary dose-response study on the effect of stevioside on TAA-induced acute liver damage, and we found that a dose of 20 mg/kg intraperitoneally afforded the best hepatoprotective effects without evident toxicity (data not shown); therefore, in this work, we decided to study the effects of stevioside on long-term TAA toxicity using this dose.

One of the main functions of the liver is to store energy in the form of glycogen; however, it is known that injured livers lose this function [31]. In this study, we found that stevioside partially preserved liver glycogen and either partially or completely prevented necrosis and cholestasis induced by TAA, providing important evidence of the beneficial properties of this compound in experimental chronic hepatic injury.

Once the liver is injured, cells from the immunological system, such as KCs and monocytes, are recruited to trigger the inflammatory process. In KCs and HSCs, NF-κB, which is the master regulator of inflammation, cell death, and wound healing in response to injury, is highly activated leading to the production and release of proinflammatory cytokines and eventually leading to fibrosis (31,32). The present results agree with previous reports in

Author Manuscript Author Manuscript Author Manuscript Author Manuscript

which stevioside was shown to downregulate NF-κB and the proinflammatory cytokines regulated by this factor (4,7,33–35), suggesting that the beneficial effects of stevioside on liver damage are associated, at least partially, with this ability.

The prooxidant and proinflammatory actions of TAA have been well established and are mainly caused by its metabolites, thioacetamide-S-oxide and thioacetamide-S-S-dioxide, which are free radicals that promote necrosis of hepatocytes and, in the long term, lead to prominent liver damage, increased oxidative stress and hepatic inflammation, similar to liver damage in humans (5). Oxidative stress plays a pivotal role in inflammatory processes, mainly by attacking polyunsaturated phospholipids in the hepatocyte cell membrane, which leads to a necrotic process that promotes the recruitment of KCs and monocytes and the release of proinflammatory cytokines that, in turn, activate quiescent HSCs. Moreover, activated macrophages produce more free radicals, such as anion superoxide, hydrogen peroxide and nitric oxide (29,36), further increasing the redox imbalance. The present results suggest that stevioside is able to maintain the normal redox state of cells, mainly by preserving the levels of Nrf2 rather than by a direct antioxidant effect as a free radical scavenger. In fact, this conclusion is supported by comparing stevioside (Fig. 5G) with a well-known free radical scavenger, quercetin (Fig. 5F). Molecules with a strong antioxidant capacity, such as quercetin, possess phenolic rings, hydroxyl groups present in catechol groups (3’ and 4’) in the B-ring, unsaturated double bonds (2,3) in the C-ring along with the 3- and 5-OH groups in the C- and A-rings, respectively, and the ability to delocalize electrons from an aromatic nucleus by a resonance effect through the 4-oxo function in the C-ring, thus conferring stability to the molecule (37). In contrast, stevioside lacks the features present in antioxidant molecules, such as quercetin but is very effective at upregulating the endogenous antioxidant system of the cell by preserving Nrf2 levels, which are responsible for regulating the expression of downstream antioxidant genes, including GPx and the redox-sensitive antioxidant glutamate cysteine ligase, which is the enzyme that catalyzes the first step of the *de novo* synthesis of GSH (38). Consistent with the literature, we found that stevioside protected the liver from oxidative stress possibly by upregulating the endogenous antioxidant machinery of the cell, counteracting the experimental liver damage.

However, it is well known that TNF-α is a cytokine that activates the NF-κB transcriptional response via TNF receptor 1 (TNFR1) and TNFR2. Thus, a pharmacological strategy to fight inflammatory diseases may be blocking TNF-α from binding to its receptors (39). Moreover, Toll-like receptors (TLRs) are pattern recognition receptors that participate in inflammatory processes by recognizing damage associated with molecular patterns. Recent data emphasize the significant impact of TLR signaling in chronic liver diseases via complex immune responses mediating HSC activation and damage (40). Notably, TLRs participate in cell injury in response to drug-induced liver injury, such as TAA (41). Thus, *in silico* results support the *in vivo* and *in vitro* findings suggesting that stevioside has an immunoregulatory because of its affinity for receptors related to the immune system, such as TLR4-MD2 and TNFR1. Naturally, the *in silico* observations must be investigated by *in vivo* and *in vitro* experiments to confirm the results predicted by the docking approach.

Author Manuscript Author Manuscript Author Manuscript Author Manuscript

In contrast to primary hepatocyte cultures that lose their ability to metabolize ethanol over time, VL17A cells express active CYP2E1 and ADH1 and are therefore similar to hepatocytes in alcoholics (6). It has been recently reported that cocultures of VL17A cells and HSCs constitute a suitable model to study alcohol-induced liver damage, which is a common disease that eventually leads to chronic hepatic injury because the metabolism of EtOH produces acetaldehyde and ROS that in turn activate HSCs (42). Thus, this coculture system represents a closer link to the *in vivo* model of TAA-induced chronic liver inflammation that shares some similarities with the human disease originating from excessive EtOH consumption. Indeed, we found that stevioside inhibited the upregulation of several genes implicated in chronic inflammation when cells were exposed to LPS or EtOH.

Conclusions

Our current results present robust evidence of the antioxidant, anti-inflammatory and immunomodulatory effects of stevioside and provide important information about the underlying mechanism of action. It is worth mentioning that stevioside shows a reasonable safety profile and may therefore be a promising tool to treat liver diseases in the clinical setting. However, further studies are necessary in animal models to provide a rationale for subsequently performing safety and short- and long-term studies in patients with hepatic pathologies.

Acknowledgments

The authors thank Rosa E. Flores-Beltrán, Laura D. Buendia-Montaño, Silvia Galindo Gómez, Karla M. Gil Becerril, Veronica Reyes Olivares, Rafael Leyva, Benjamín E. Chavez, and Ricardo Gaxiola for their excellent technical assistance. The authors also acknowledge the Animal Lab Facility, UPEAL-Cinvestav and Dr. Jorge Fernández-Hernández.

Statement of financial support:

This research was supported by the National Council of Science and Technology (Conacyt) of Mexico, grant No. 253037 to Muriel P, by fellowship No. 355795 to Sael Casas-Grajales from Conacyt, and by the NIAAA/NIH grant No. K01AA025140–02 to Karina Reyes-Gordillo.

6 References

[1]. Ragone MI, Bonazzola P, Colareda GA, Lazarte ML, Bruno F, Consolini AE, Cardioprotection of stevioside on stunned rat hearts: A mechano-energetical study, Phytomedicine. 35 (2017) 18–26. doi:10.1016/j.phymed.2017.08.022. [PubMed: 28991641]

[2]. Ilić V, Vukmirović S, Stilinović N, Čapo I, Arsenović M, Milijašević B, Insight into anti-diabetic effect of low dose of stevioside, Biomed. Pharmacother 90 (2017) 216–221. doi:10.1016/j.biopha.2017.03.045. [PubMed: 28363166]

[3]. Panagiotou C, Mihailidou C, Brauhli G, Katsarou O, Moutsatsou P, Effect of steviol, steviol glycosides and stevia extract on glucocorticoid receptor signaling in normal and cancer blood cells, Mol. Cell. Endocrinol 460 (2018) 189–199. doi:10.1016/j.mce.2017.07.023. [PubMed: 28754349]

[4]. Wang Z, Xue L, Guo C, Han B, Pan C, Zhao S, Song H, Ma Q, Stevioside ameliorates high-fat diet-induced insulin resistance and adipose tissue inflammation by downregulating the NF-κB pathway, Biochem. Biophys. Res. Commun 417 (2012) 1280–1285. doi:10.1016/j.bbrc.2011.12.130. [PubMed: 22240021]

[5]. Muriel P, Ramos-Tovar E, Montes-Páez G, Buendía-Montaño LD, Experimental models of liver damage mediated by oxidative stress, in: Muriel P (Ed.), Liver Pathophysiology: Therapies &

Author Manuscript Author Manuscript Author Manuscript Author Manuscript

Antioxidants, Elsevier, Waltham, MA, USA, 2017: pp. 529–546. doi:10.1016/B978-0-12-804274-8.00040-0.

[6]. Donohue TM, Osna NA, Clemens DL, Recombinant Hep G2 cells that express alcohol dehydrogenase and cytochrome P450 2E1 as a model of ethanol-elicited cytotoxicity, Int. J. Biochem. Cell Biol. 38 (2006) 92–101. doi:10.1016/j.biocel.2005.07.010. [PubMed: 16181800]

[7]. L. S, Chaudhary S, R. RS, Hydroalcoholic extract of Stevia rebaudiana bert. leaves and stevioside ameliorates lipopolysaccharide induced acute liver injury in rats, Biomed. Pharmacother 95 (2017) 1040–1050. doi:10.1016/j.biopha.2017.08.082. [PubMed: 28922721]

[8]. Nakamura A, Ueno T, Yagi Y, Okuda K, Ogata T, Nakamura T, Torimura T, Iwamoto H, Ramadoss S, Sata M, Tsutsumi V, Yasuda K, Tomiyasu Y, Obayashi K, Tashiro K, Kuhara S, Human primary cultured hepatic stellate cells can be cryopreserved, Med. Mol. Morphol 43 (2010) 107–115. doi:10.1007/s00795-009-0484-5. [PubMed: 20683699]

[9]. Reyes-Gordillo K, Shah R, Popratiloff A, Fu S, Hindle A, Brody F, Rojkind M, Thymosin-β4 (Tβ4) blunts PDGF-dependent phosphorylation and binding of AKT to actin in hepatic stellate cells, Am. J. Pathol 178 (2011) 2100–2108. doi:10.1016/j.ajpath.2011.01.025. [PubMed: 21514425]

[10]. Geerts A, History, heterogeneity, developmental biology, and functionsof quiescent hepatic stellate cells, Semin. Liver Dis. 21 (2001) 311–335. [PubMed: 11586463]

[11]. Arellanes-Robledo J, Reyes-Gordillo K, Ibrahim J, Leckey L, Shah R, Lakshman MR, Ethanol targets nucleoredoxin/dishevelled interactions and stimulates phosphatidylinositol 4-phosphate production in vivo and in vitro, Biochem. Pharmacol 156 (2018) 135–146. doi:10.1016/j.bcp.2018.08.021. [PubMed: 30125555]

[12]. Reitman S, Frankel S, A colorimetric method for the determination of serum glutamic oxalacetic and glutamic pyruvic transaminases, Am. J. Clin. Pathol 28 (1957) 56–63.

[13]. Glossmann H, Neville DM, gamma-Glutamyltransferase in kidney brush border membranes, FEBS Lett. 19 (1972) 340–344. [PubMed: 11946246]

[14]. Bergmeyer HU, Marianne G, Walter HE, Enzymes, in: Bergmeyer J, Marianne G (Eds.), Methods Enzym. Anal, Verlag-Chemie, Weinheim, Baden-Württemberg, Germany, 1983: pp. 269–270.

[15]. Seifter S, Dayton S, Novic B, Muntwyler E, The estimation of glycogen with the anthrone reagent, Arch. Biochem 25 (1950) 191–200. [PubMed: 15401229]

[16]. Casas-Grajales S, Alvarez-Suarez D, Ramos-Tovar E, Buendía-Montaño LD, Reyes-Gordillo K, Camacho J, Tsutsumi V, Lakshman MR, Muriel P, Stevioside inhibits experimental fibrosis by down-regulating profibrotic Smad pathways and blocking hepatic stellate cell activation, Basic Clin. Pharmacol. Toxicol In press (2019) 1–11. doi:10.1111/bcpt.13194.

[17]. Casas-Grajales S, Vázquez-Flores LF, Ramos-Tovar E, Hernández-Aquino E, Flores-Beltrán RE, Cerda-García-Rojas CM, Camacho J, Shibayama M, Tsutsumi V, Muriel P, Quercetin reverses experimental cirrhosis by immunomodulation of the proinflammatory and profibrotic processes, Fundam. Clin. Pharmacol 31 (2017) 610–624. doi:10.1111/fcp.12315. [PubMed: 28802065]

[18]. Ohkawa H, Ohishi N, Yagi K, Assay for lipid peroxides in animal tissues by thiobarbituric acid reaction, Anal. Biochem 95 (1979) 351–358. doi:10.1016/0003-2697(79)90738-3. [PubMed: 36810]

[19]. Bradford MM, A rapid and sensitive method for the quantitation of microgram quantities of protein utilizing the principle of protein-dye binding, Anal. Biochem 72 (1976) 248–254. doi:10.1016/0003-2697(76)90527-3. [PubMed: 942051]

[20]. Livak KJ, Schmittgen TD, Analysis of relative gene expression data using real-time quantitative PCR and the 2-ΔΔCT method, Methods. 25 (2001) 402–408. doi:10.1006/meth.2001.1262. [PubMed: 11846609]

[21]. Ahmed J, Preissner S, Dunkel M, Worth CL, Eckert A, Preissner R, SuperSweet-A resource on natural and artificial sweetening agents, Nucleic Acids Res. 39 (2011) 377–382. doi:10.1093/nar/gkq917.

[22]. Hanwell MD, Curtis DE, Lonie DC, Vandermeerschd T, Zurek E, Hutchison GR, Avogadro: An advanced semantic chemical editor, visualization, and analysis platform, J. Cheminform 4 (2012) 1–17. doi:10.1186/1758-2946-4-17. [PubMed: 22236646]

Author Manuscript Author Manuscript Author Manuscript Author Manuscript

[23]. Halgren TA, Merck molecular force field. I. Basis, form, scope, parameterization, and performance of MMFF94*, J. Comput. Chem 17 (1996) 490–519. doi:10.1002/(SICI)1096-987X(199604)17:5/6<520::AID-JCC2>3.0.CO;2-W.

[24]. Frisch MJ, Trucks GW, Schlegel HB, Scuseria GE, Robb MA, Cheeseman JR, Scalmani G, Barone V, Petersson GA, Nakatsuji H, Li X, Caricato M, Marenich A, Bloino J, Janesko BG, Gomperts R, Mennucci B, Hratchian HP, Ortiz JV, Izmaylov AF, Sonnenberg JL, Williams-Young D, Ding F, Lipparini F, Egidi F, Goings J, Peng B, Petrone A, Henderson T, Ranasinghe D, Zakrzewski VG, Gao J, Rega N, Zheng G, Liang W, Hada M, Ehara M, Toyota K, Fukuda R, Hasegawa J, Ishida M, Nakajima T, Honda Y, Kitao O, Nakai H, Vreven T, Throssell K, Montgomery JA, Peralta JE, Ogliaro F, Bearpark M, Heyd JJ, Brothers E, Kudin KN, Staroverov VN, Keith T, Kobayashi R, Normand J, Raghavachari K, Rendell A, Burant JC, Iyengar SS, Tomasi J, Cossi M, Millam JM, Klene M, Adamo C, Cammi R, Ochterski JW, Martin RL, Morokuma K, Farkas O, Foresman JB, Fox DJ, Gaussian 09W, (2016). http://gaussian.com/.

[25]. Morris GM, Huey R, Lindstrom W, Sanner MF, Belew RK, Goodsell DS, Olson AJ, AutoDock4 and AutoDockTools4: Automated docking with selective receptor flexibility, J. Comput. Chem 30 (2009) 2785–2791. doi:10.1002/jcc.21256.AutoDock4. [PubMed: 19399780]

[26]. Kim HM, Park BS, Kim J-I, Kim SE, Lee J, Oh SC, Enkhbayar P, Matsushima N, Lee H, Yoo OJ, Lee J-O, Crystal structure of the TLR4-MD-2 complex with bound endotoxin antagonist Eritoran, Cell. 130 (2007) 906–917. doi:10.1016/j.cell.2007.08.002. [PubMed: 17803912]

[27]. Carter PH, Scherle PA, Muckelbauer JA, Voss ME, Liu R-Q, Thompson LA, Tebben AJ, Solomon KA, Lo YC, Li Z, Strzemienski P, Yang G, Falahatpisheh N, Xu M, Wu Z, Farrow NA, Ramnarayan K, Wang J, Rideout D, Yalamoori V, Domaille P, Underwood DJ, Trzaskos JM, Friedman SM, Newton RC, Decicco CP, Photochemically enhanced binding of small molecules to the tumor necrosis factor receptor-1 inhibits the binding of TNF-a, Proc. Natl. Acad. Sci. U. S. A 98 (2001) 11879–11884. doi:10.1073/pnas.211178398. [PubMed: 11592999]

[28]. Kershenobich D, Gutiérrez-Reyes DG, Is human cirrhosis a reversible disease?, in: Muriel P (Ed.), Liver Pathophysiology: Therapies & Antioxidants, Elsevier, Waltham, MA, USA, 2017: pp. 259–265. doi:10.1016/B978-0-12-804274-8.00019-9.

[29]. Casas-Grajales S, Muriel P, The liver, oxidative stress, and antioxidants, in: Muriel P (Ed.), Liver Pathophysiology: Therapies & Antioxidants, Elsevier, Waltham, MA, USA, 2017: pp. 583–604. doi:10.1016/B978-0-12-804274-8.00043-6.

[30]. Meng X-Y, Zhang H-X, Mezei M, Cui M, Molecular docking: a powerful approach for structure-based drug discovery., Curr. Comput. Aided. Drug Des. 7 (2011) 146–157. doi:10.2174/157340911795677602. [PubMed: 21534921]

[31]. Elsharkawy AM, Mann DA, Nuclear factor-κB and the hepatic inflammation-fibrosis-cancer axis, Hepatology. 46 (2007) 590–597. doi:10.1002/hep.21802. [PubMed: 17661407]

[32]. Luedde T, Schwabe RF, NF-κB in the liver-linking injury, fibrosis and hepatocellular carcinoma, Nat. Rev. Gastroenterol. Hepatol 8 (2011) 108–118. doi:10.1038/nrgastro.2010.213. [PubMed: 21293511]

[33]. Wang T, Guo M, Song X, Zhang Z, Jiang H, Wang W, Fu Y, Cao Y, Zhu L, Zhang N, Stevioside plays an anti-inflammatory role by regulating the NF-κB and MAPK pathways in S. aureus-infected mouse mammary glands, Inflammation. 37 (2014) 1837–1846. doi:10.1007/s10753-014-9915-0. [PubMed: 24858724]

[34]. Boonkaewwan C, Burodom A, Anti-inflammatory and immunomodulatory activities of stevioside and steviol on colonic epithelial cells, J. Sci. Food Agric 93 (2013) 3820–3825. doi:10.1002/jsfa.6287. [PubMed: 23794454]

[35]. Boonkaewwan C, Toskulkao C, Vongsakul M, Anti-inflammatory and immunomodulatory activities of stevioside and its metabolite steviol on THP-1 cells, J. Agric. Food Chem. 54 (2006) 785–789. doi:10.1021/jf0523465. [PubMed: 16448183]

[36]. Casas-Grajales S, Muriel P, Antioxidants in liver health, World J. Gastrointest. Pharmacol. Ther 6 (2015) 59–72. doi:10.4292/wjgpt.v6.i3.59. [PubMed: 26261734]

[37]. Vázquez-Flores LF, Casas-Grajales S, Hernández-Aquino E, Vargas-Pozada EE, Muriel P, Antioxidant, antiinflammatory, and antifibrotic properties of quercetin in the liver, in: Muriel P (Ed.), Liver Pathophysiology: Therapies & Antioxidants, Elsevier, Waltham, MA, USA, 2017: pp. 653–674. doi:10.1016/B978-0-12-804274-8.00047-3.

Author Manuscript Author Manuscript Author Manuscript Author Manuscript

[38]. Zhang Q, Pi J, Woods CG, Andersen ME, A systems biology perspective on Nrf2-mediated antioxidant response, Toxicol. Appl. Pharmacol 244 (2010) 84–97. doi:10.1016/j.taap.2009.08.018. [PubMed: 19716833]

[39]. Ting AT, Bertrand MJM, More to life than NF-κB in TNFR1 signaling, Trends Immunol. 37 (2016) 535–545. doi:10.1016/j.it.2016.06.002. [PubMed: 27424290]

[40]. Kiziltas S, Toll-like receptors in pathophysiology of liver diseases, World J. Hepatol 8 (2016) 1354–1369. doi:10.4254/wjh.v8.i32.1354. [PubMed: 27917262]

[41]. Kuramochi M, Izawa T, Pervin M, Bondoc A, Kuwamura M, Yamate J, The kinetics of damage-associated molecular patterns (DAMPs) and toll-like receptors during thioacetamide-induced acute liver injury in rats, Exp. Toxicol. Pathol 68 (2016) 471–477. doi:10.1016/j.etp.2016.06.005. [PubMed: 27522298]

[42]. Casini A, Pellegrini G, Ceni E, Salzano R, Parola M, Robino G, Milani S, Dianzani MU, Surrenti C, Human hepatic stellate cells express class I alcohol dehydrogenase and aldehyde dehydrogenase but not cytochrome P4502E1., J. Hepatol 28 (1998) 40–5. [PubMed: 9537862]

Author Manuscript Author Manuscript Author Manuscript Author Manuscript

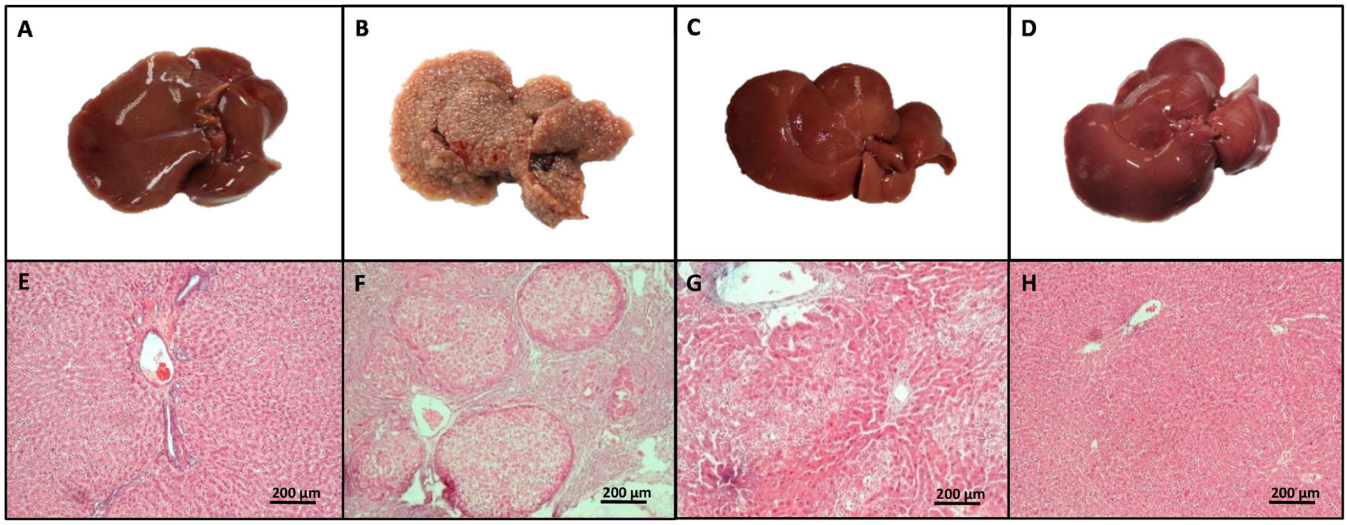

Figure 1. Stevioside prevents the macroscopic structure formation and H&E trichrome staining in livers from TAA-treated rats.

The effect of stevioside (STV) on the macroscopic structure and on hematoxylin and eosin staining in the livers of control rats (A, E), TAA-treated rats (B, F), STV+TAA-treated rats (C, G) and rats administered STV alone (D, H).

Author Manuscript Author Manuscript Author Manuscript Author Manuscript

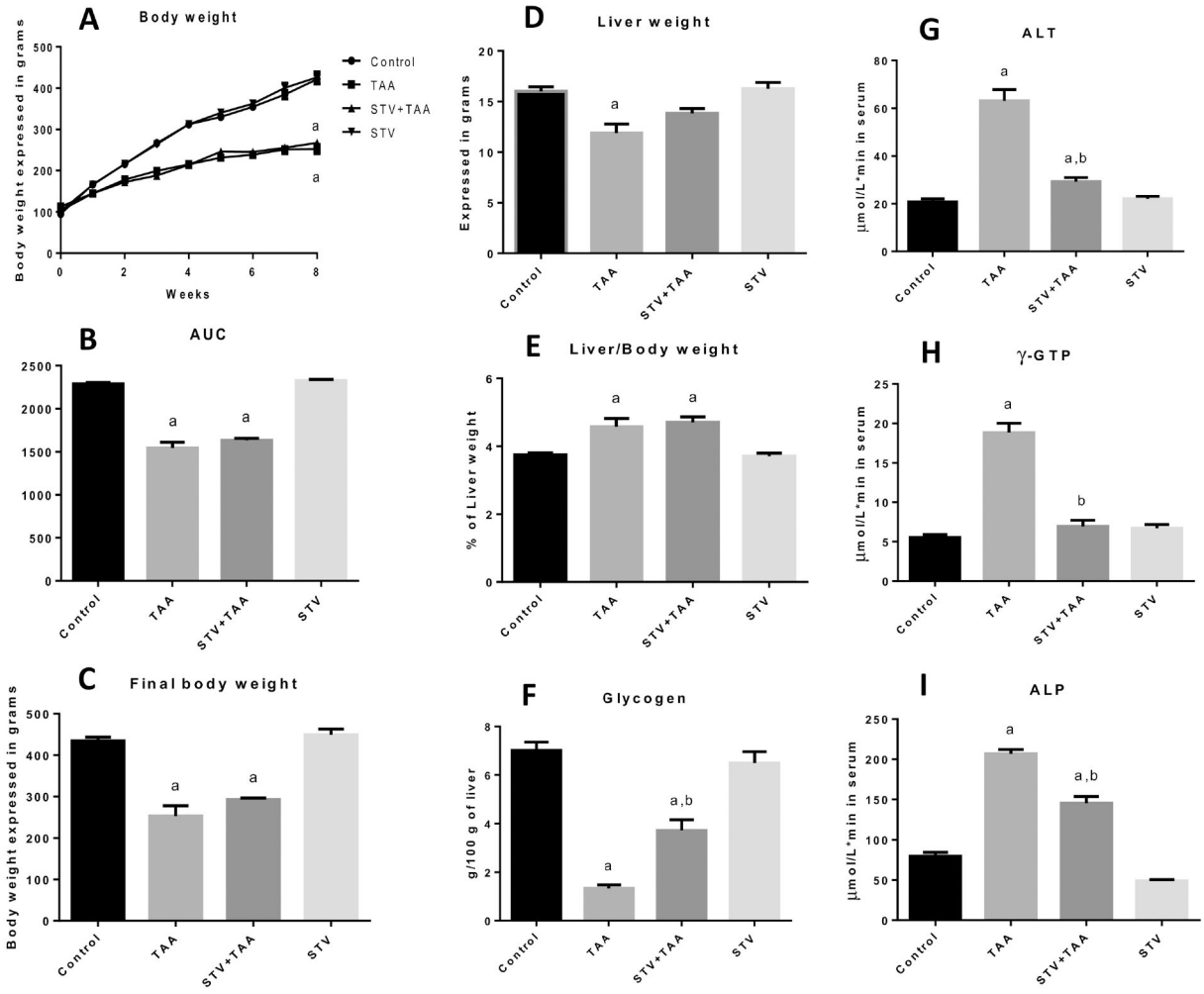

Figure 2. Stevioside (STV) prevents liver damage induced by chronic thioacetamide (TAA) administration to rats.

Histograms depict body weight gain (A), area under the curve (B), final body weight (C), liver weight (D), liver/body weight ratio (E), liver glycogen content (F), and serum activities of ALT (G), γ-GTP (H), and ALP (I). Each bar represents the mean value of experiments performed in duplicate assays ± SEM ($n = 8$). [a]$p < 0.05$ vs control. [b]$p < 0.05$ vs TAA.

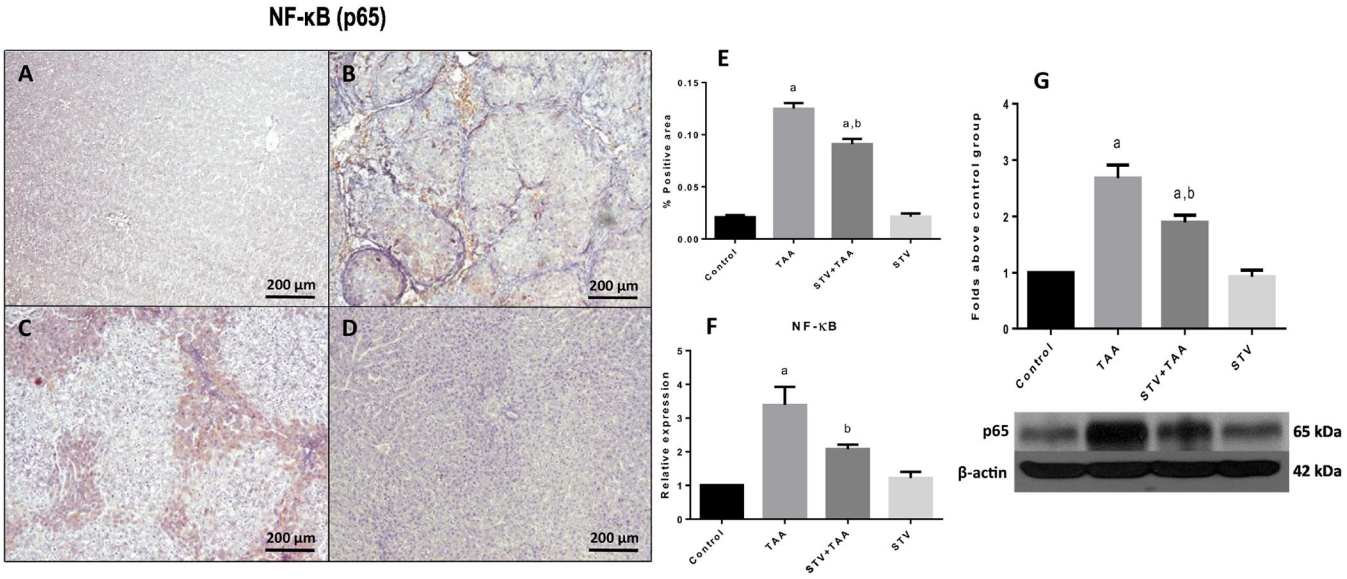

Figure 3. Immunomodulatory effect of stevioside (STV) in injured livers.

Representative p65 immunohistochemistry obtained from livers of control rats (A), TAA-treated rats (B), STV+TAA-treated rats (C), and rats administered STV alone (D). The histogram depicts the percentage of p65 positivity obtained in immunohistochemistry sections (E). Increases in relative mRNA expression and protein levels of p65 (F, G) are shown. β-Actin was used as a control. Each bar represents the mean value of experiments conducted in duplicate assays ± SEM ($n = 3$). $^{a}p < 0.05$ vs control. $^{b}p < 0.05$ vs TAA.

Author Manuscript Author Manuscript Author Manuscript Author Manuscript

Author Manuscript Author Manuscript Author Manuscript Author Manuscript

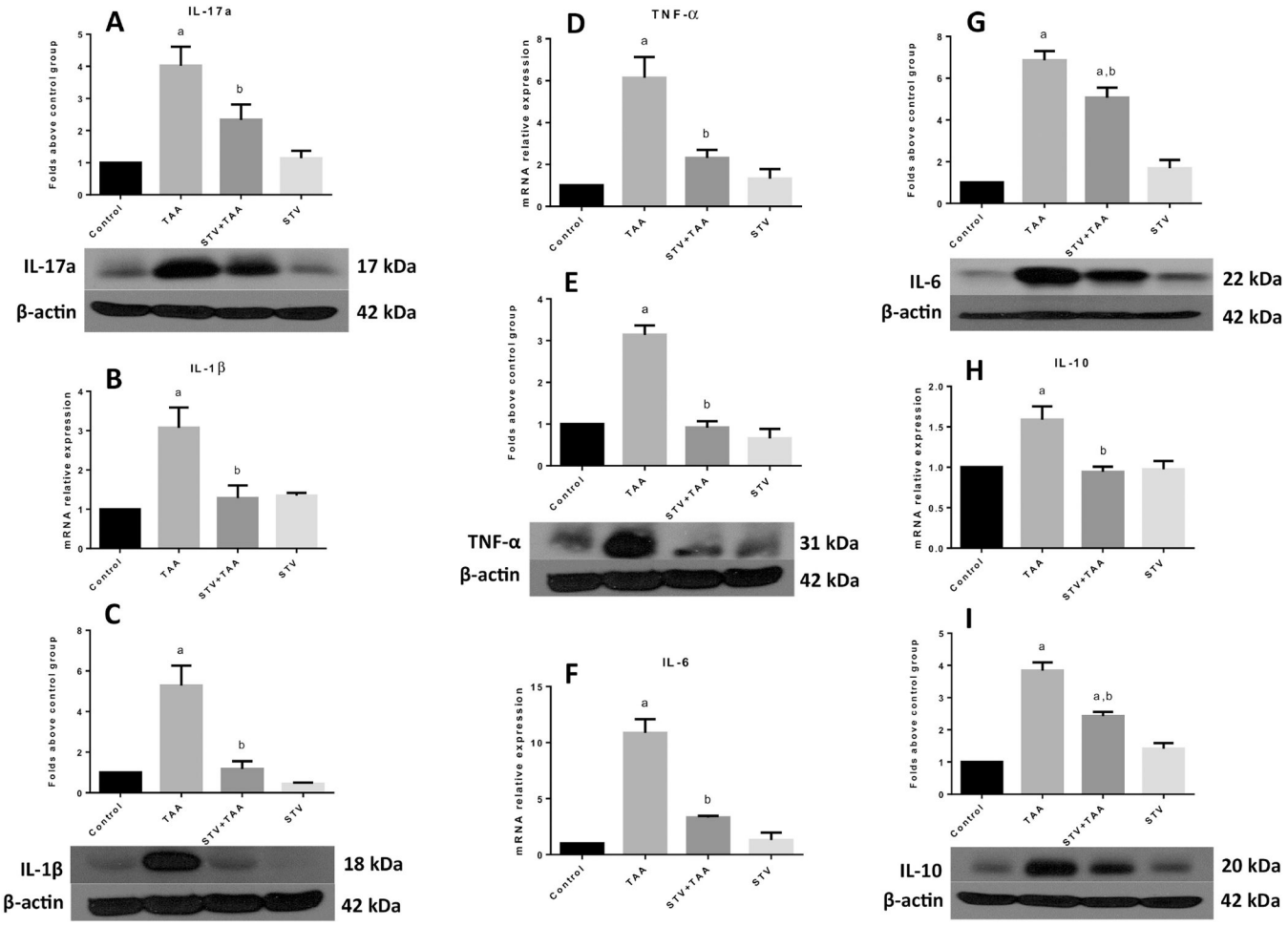

Figure 4. Stevioside (STV) prevents the production of proinflammatory cytokines in thioacetamide (TAA)-induced cirrhosis.

Protein levels of IL-17a (A), mRNA and protein level increase of IL-1β (B, C), TNF-α (D, E), IL-6 (F, G) and IL-10 (H, I) are shown. β-Actin was used as a control. The values are expressed as the fold increase of optical densitometry normalized to the control group values (control = 1). Each bar represents the mean value of experiments conducted in duplicate assays ± SEM ($n = 3$). [a]$p < 0.05$ vs control. [b]$p < 0.05$ vs TAA.

Author Manuscript Author Manuscript Author Manuscript Author Manuscript

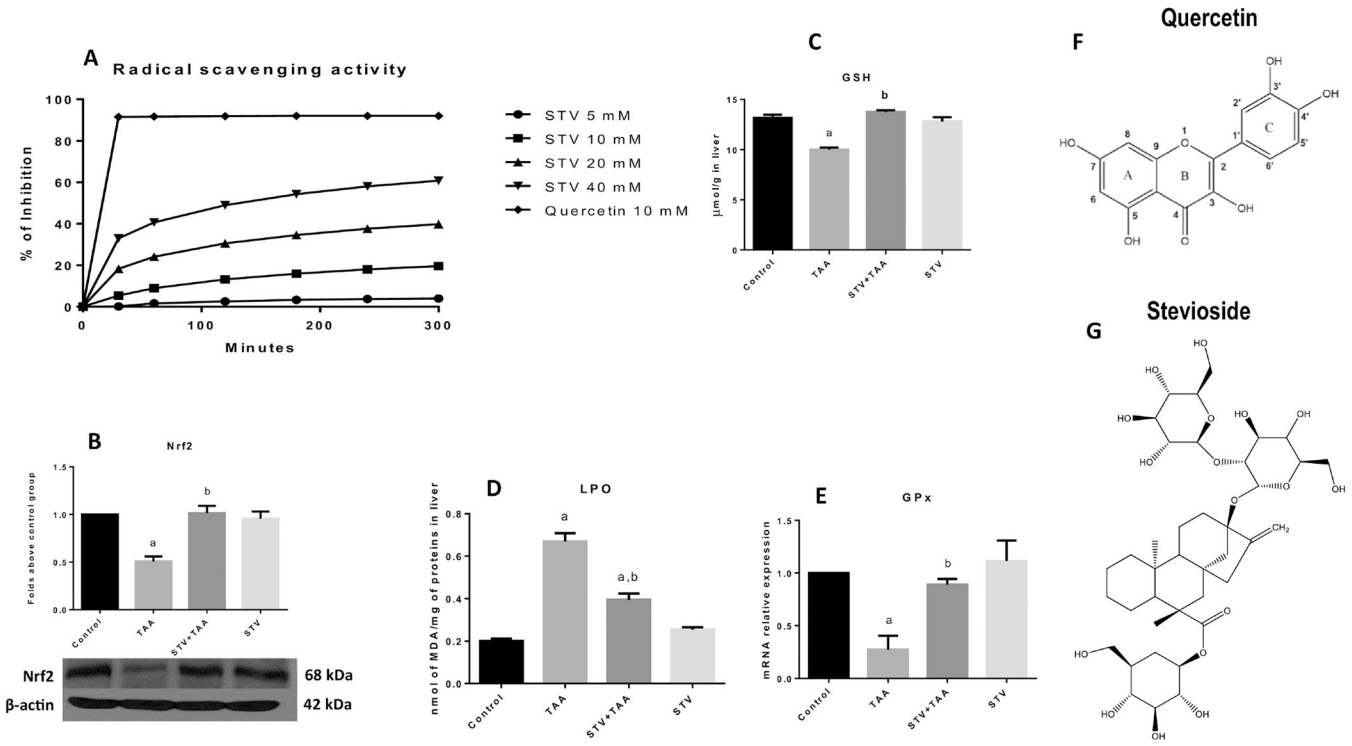

Figure 5. Effect of stevioside on the redox system.

The effect of stevioside (SVT) at 5, 10, 20 and 40 mM on radical scavenging activity (RSA) using DPPH˙ as a free radical (A). Western blot analysis of Nrf2 (B) in samples of liver tissue from control, thioacetamide (TAA)-treated, STV + TAA-treated, and stevioside-only treated rats. β-Actin was used as a control. The values are expressed as the fold increase of optical densitometry normalized to the control group values ($n = 3$). GSH (C) and lipid peroxidation (LPO) (D) are shown (n=8). Each bar represents the mean value of experiments conducted in duplicate assays ± SEM ($n = 8$). The increase in relative mRNA expression of GPx (E) is shown (n=3). Each bar represents the mean value of experiments conducted in duplicate assays ± SEM. $^{a}p < 0.05$ vs control. $^{b}p < 0.05$ vs TAA. Representation of the chemical structures of quercetin (F) and stevioside (G).

Author Manuscript Author Manuscript Author Manuscript Author Manuscript

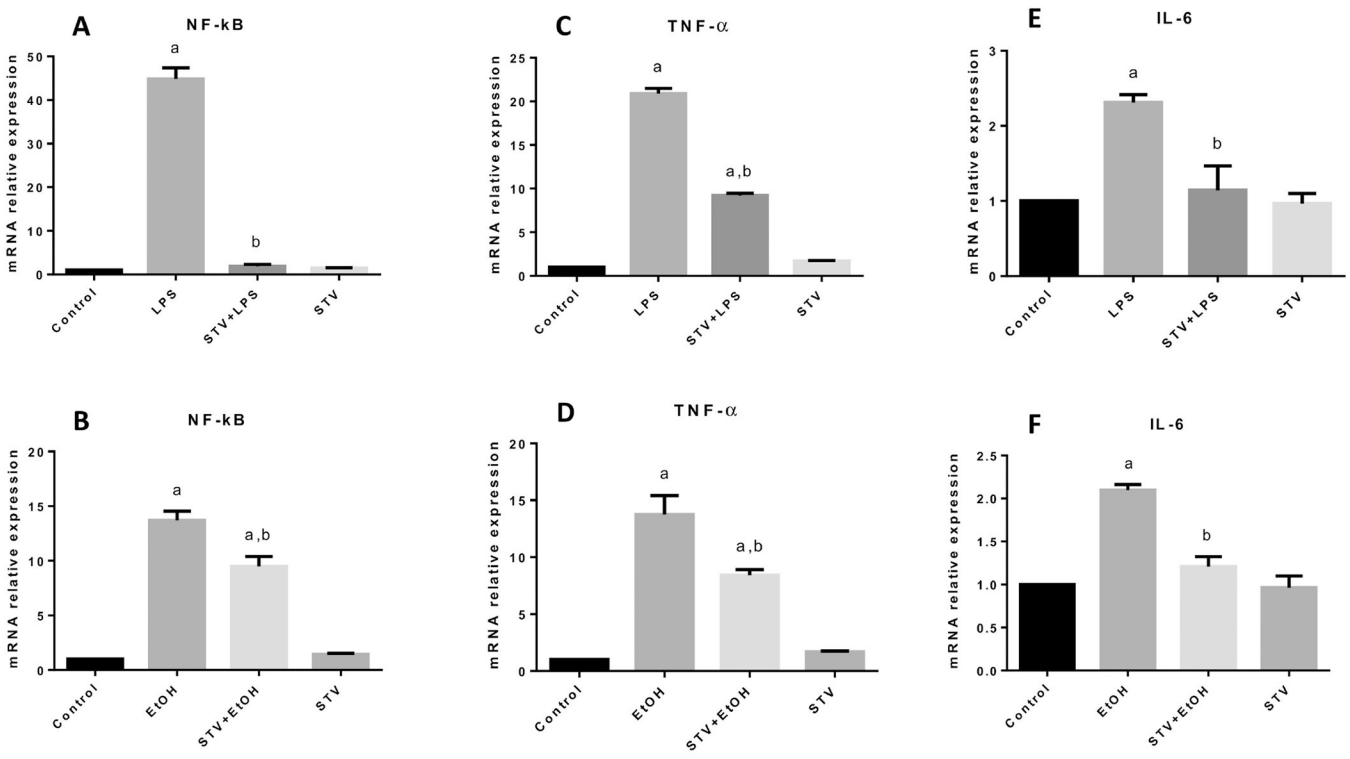

Figure 6. The immunomodulatory effect of stevioside (STV) in cocultured cells.

Increases in relative mRNA expression of NF-κB (A, B); TNF-α (C, D); and IL-6 (E, F) in samples of cocultured hHSC and VL-17A cell lines from control, LPS and EtOH-treated, STV + LPS or EtOH-treated, and STV-only treated cocultured cells are shown. β-Actin was used as a control. Each bar represents the mean value of experiments conducted in duplicate assays ± SEM ($n = 3$). [a]$p < 0.05$ vs control. [b]$p < 0.05$ vs TAA.

Author Manuscript Author Manuscript Author Manuscript Author Manuscript

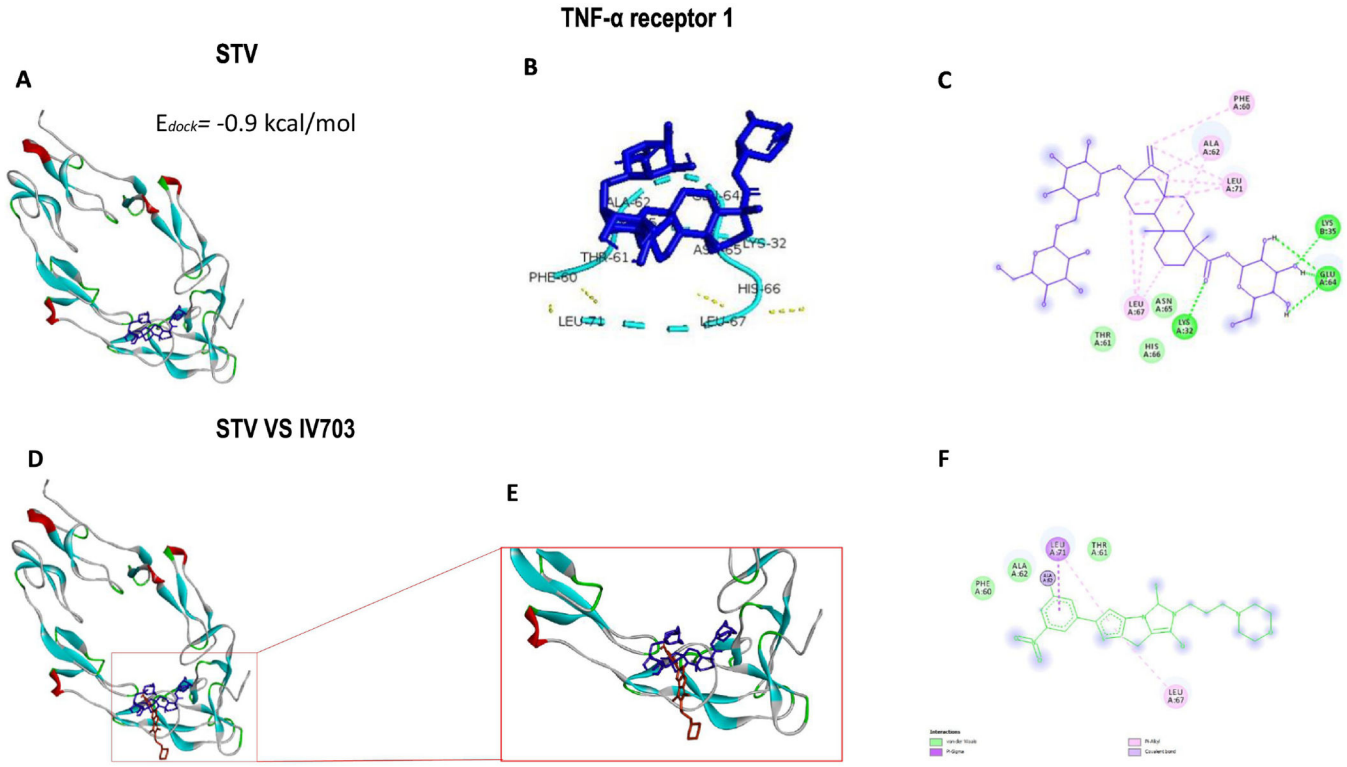

Figure 7. Stevioside (STV) docking with the TNF-α receptor 1.

The binding energy of STV docked to TNFR1 (A). STV interactions with amino acids at the active site of TNFR1 (B). The 2D view of STV interactions with amino acids (C). Overlay of STV and the IV703 ligand at the active site of TNFR1 (D). Enlargement of the stevioside-IV703 overlay (E). The 2D view of the IV703 interaction with amino acids at the active site of TNFR1 (F).

Author Manuscript
Author Manuscript
Author Manuscript
Author Manuscript

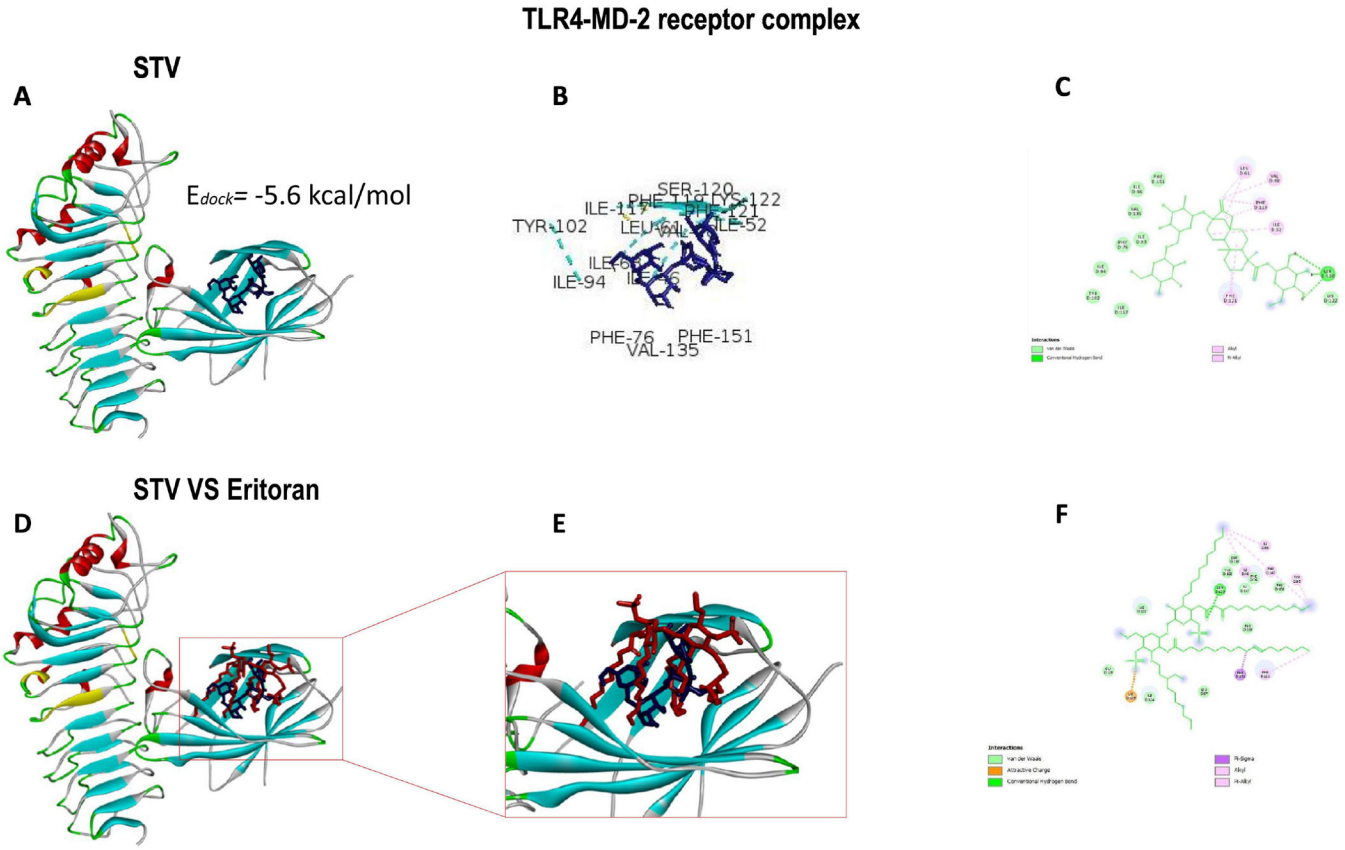

Figure 8. Stevioside (STV) docking with the TLR4-MD2 receptor complex.

The binding energy of STV docked with the TLR4-MD2 complex (A). STV interactions with amino acids at the active site of the TLR4-MD2 complex (B). The 2D view of the STV interactions with amino acids (C). Overlay of STV and the Eritoran ligand at the active site of the TLR4-MD2 complex (D). Enlargement of the STV-Eritoran overlay (E). The 2D view of the Eritoran interaction with amino acids at the active site of the TLR4-MD2 complex (F).

Author Manuscript

Author Manuscript

Author Manuscript

Author Manuscript

Table 1.

Complete list of antibodies used in Western blot and immunohistochemistry assays.

Protein	Catalog number	Brand
IL-6	ARC0962	Invitrogen (Waltham, MA, USA)
IL-10	ARC9102	
Goat anti-mouse IgG (H+L), HRP	62–6520	
TGF-β1	05–1423	
TNF-α	SC-52746	Santa Cruz (Santa Cruz, CA, USA)
α-SMA	A5691	
Nrf2	ab31163	
Smad7	ab90086	
Goat anti-rabbit IgG (H+L), HRP	ab6721	
β-actin	AM4302	Ambion (Austin, TX, USA)
NF-κB (p65)	MAB3026	Merck Millipore (Burlington, MA, USA)
MMP-13	MAB13426	

Author Manuscript Author Manuscript Author Manuscript Author Manuscript

Table 2.

Genes studied and probes used in the *in vitro* qRT-PCR experiments.

Target	NCBI Reference sequence	Forward primer	Reverse primer	Product length
hIL-6	NM_000600.4	5′-AAA GAG GCA CTG GCA GAA AA-3′	5′-TTT CAC CAG GCA AGT CTC CT-3′	99 bp
hIL-1β	NM_000576.2	5′-ATG CAC CTG TAC GAT CAC TGA-3′	5′-ACA AAG GAC ATG GAG AAC ACC-3′	142 bp
hNF-κB (p65/RelA)	NM_021975.3	5′-AAT GGC TCG TCT GTA GTG C-3′	5′-TGC TCA ATG ATC TCC ACA TAG G-3′	145 bp
hTNF-α	NM_000594.3	5′-ACT TTG GAG TGA TCG GCC-3′	5′-GCT TGA GGG TTT GCT ACA AC-3′	139 bp
hα-SMA (Acta2)	NM_001141945.2	5′-CTG AGC GTG GCT ATT CCT TC-3′	5′-GCA GTG GCC ATC TCA TTT TC-3′	109 bp
hPDGF-β receptor	NM_002609.3	5′-GGC TAC ATG GAC ATG AGC AA-3′	5′-TCG GCA GGT CCT CTC AG-3′	150 bp
hSMAD3 (MADH3)	NM_005902.3	5′-GGA GAA ATG GTG CGA GAA GG-3′	5′-GAA GGC GAA CTC ACA CAG C-3′	259 bp
hTGF-β1	NM_000660.6	5′-TGA ACC GGC CTT TCC TGC TTC TCA TG-3′	5′-GCG GAA GTC AAT GTA CAG CTG CCG C-3′	152 bp
hPPAR-γ	NM_138712.3	5′-GCT GGC CTC CTT GAT GAA TA-3′	5′-TTG GGC TCC ATA AAG TCA CC-3′	114 bp
c-Myc	NM_002467.5	5′-TCA AGA GGC GAA CAC ACA AC-3′	5′-GGC CTT TTC ATT GTT TTC CA-3′	110 bp
hβ-actin (ACTB)	NM_001101.4	5′-GGA GAA TGG CCC AGT CCT C-3′	5′-GGG CAC GAA GGC TCA TCA T-3′	145 bp